blood

2013 122: 958-968
Prepublished online June 27, 2013;
doi:10.1182/blood-2013-01-482026

Integrated phosphoproteomic and metabolomic profiling reveals NPM-ALK –mediated phosphorylation of PKM2 and metabolic reprogramming in anaplastic large cell lymphoma

Scott R. P. McDonnell, Steven R. Hwang, Delphine Rolland, Carlos Murga-Zamalloa, Venkatesha Basrur, Kevin P. Conlon, Damian Fermin, Thomas Wolfe, Alexander Raskind, Chunhai Ruan, Jian-Kang Jiang, Craig J. Thomas, Cory M. Hogaboam, Charles F. Burant, Kojo S. J. Elenitoba-Johnson and Megan S. Lim

Blood (print ISSN 0006-4971, online ISSN 1528-0020), is published weekly by the American Society of Hematology, 2021 L St, NW, Suite 900, Washington DC 20036.

LYMPHOID NEOPLASIA

Integrated phosphoproteomic and metabolomic profiling reveals NPM-ALK–mediated phosphorylation of PKM2 and metabolic reprogramming in anaplastic large cell lymphoma

Scott R. P. McDonnell,[1] Steven R. Hwang,[1] Delphine Rolland,[1] Carlos Murga-Zamalloa,[1] Venkatesha Basrur,[1] Kevin P. Conlon,[1] Damian Fermin,[1] Thomas Wolfe,[1] Alexander Raskind,[2] Chunhai Ruan,[2] Jian-Kang Jiang,[3] Craig J. Thomas,[3] Cory M. Hogaboam,[1] Charles F. Burant,[2] Kojo S. J. Elenitoba-Johnson,[1] and Megan S. Lim[1]

Departments of [1]Pathology and [2]Internal Medicine, University of Michigan, Ann Arbor, MI; and [3]National Institutes of Health Chemical Genomics Center, National Center for Advancing Translational Sciences, National Institutes of Health, Bethesda, MD

Key Points

- NPM-ALK induces a metabolic shift toward biomass production.
- NPM-ALK phosphorylates Y105-PKM2 to regulate metabolism and tumorigenesis.

The mechanisms underlying the pathogenesis of the constitutively active tyrosine kinase *nucleophosmin-anaplastic lymphoma kinase* (NPM-ALK) expressing anaplastic large cell lymphoma are not completely understood. Here we show using an integrated phosphoproteomic and metabolomic strategy that NPM-ALK induces a metabolic shift toward aerobic glycolysis, increased lactate production, and biomass production. The metabolic shift is mediated through the anaplastic lymphoma kinase (ALK) phosphorylation of the tumor-specific isoform of pyruvate kinase (PKM2) at Y105, resulting in decreased enzymatic activity. Small molecule activation of PKM2 or expression of Y105F PKM2 mutant leads to reversal of the metabolic switch with increased oxidative phosphorylation and reduced lactate production coincident with increased cell death, decreased colony formation, and reduced tumor growth in an in vivo xenograft model. This study provides comprehensive profiling of the phosphoproteomic and metabolomic consequences of NPM-ALK expression and reveals a novel role of ALK in the regulation of multiple components of cellular metabolism. Our studies show that PKM2 is a novel substrate of ALK and plays a critical role in mediating the metabolic shift toward biomass production and tumorigenesis. (*Blood*. 2013;122(6):958-968)

Introduction

Anaplastic large cell lymphoma (ALCL) is a subtype of peripheral T-cell lymphoma representing 3% of adult non-Hodgkin lymphomas and 10% to 15% of all childhood lymphomas.[1] A significant proportion of pediatric ALCLs (~80%) is characterized by the recurrent t(2;5)(p23;q35) chromosomal aberration that juxtaposes anaplastic lymphoma kinase (ALK) and nucleophosmin (NPM). This chimeric fusion generates the constitutively active tyrosine kinase (NPM-ALK) that drives oncogenesis in ALCLs.[2] Structural alterations targeting *ALK* including translocations, amplifications, and point mutations have been identified in diverse neoplasia comprising non–small cell lung cancer, inflammatory myofibroblastic tumors, and neuroblastoma.[3-5] The oncogenic potential of ALK has been demonstrated by its ability to activate numerous canonical growth factor signaling pathways including phosphoinositide 3-kinase/AKT, Janus kinase/signal transducer and activator of transcription, and phospholipase C-γ.[6-11]

Cellular reprogramming of energy metabolism is an emerging hallmark of cancer.[12] Metabolic reprogramming via the "Warburg effect" is characterized by alternate glycolysis and increased lactate production even in the presence of abundant oxygen.[13] Although resting cells need to continuously produce energy, proliferating cells shift their metabolism toward biomass (nucleic acids, amino acids, lipids) production to accumulate material for further replication.[14]

To identify novel proteins/pathways that mediate ALK signaling, we used a phosphoproteomic study that revealed numerous metabolic proteins to be regulated by ALK. Therefore, we pursued a mass spectrometry (MS)–based metabolomic study to characterize the ALK-driven metabolic signature. Integrated analysis of the phosphoproteomic and metabolomic studies led to the discovery and characterization of an ALK-induced metabolic switch. Our results show that the tumor-specific isoform of pyruvate kinase (PKM2) is a novel substrate of NPM-ALK and plays a key role in promotion of the Warburg effect. Small molecule activators of PKM2 or expression of a PKM2 mutant (Y105F-PKM2) resulted in a reversal of the metabolic shift and decreased tumorigenesis of ALK^+ ALCL cells. These studies reveal a novel role of ALK in the regulation of cellular metabolism via the phosphorylation of PKM2 and offer a rationale for PKM2 activators as potential therapeutic agents for ALK^+ ALCL.

Methods

Details relating to phosphoproteomics, metabolomics, metabolomic pathway analysis, and metabolic flux are provided in the supplemental Methods on the *Blood* website.

Submitted January 30, 2013; accepted June 14, 2013. Prepublished online as *Blood* First Edition paper, June 27, 2013; DOI 10.1182/blood-2013-01-482026.

The online version of this article contains a data supplement.

The publication costs of this article were defrayed in part by page charge payment. Therefore, and solely to indicate this fact, this article is hereby marked "advertisement" in accordance with 18 USC section 1734.

Cell culture

ALCL-derived cell lines (SU-DHL-1, DEL, Karpas299, SUPM2) were maintained in RPMI-1640 with 10% fetal bovine serum. Stable cell lines were generated with lentiviral transduction and puromycin selection.

Compounds

ALK inhibitor CEP-26939 (CEP) was acquired from Cephalon.[15] PKM2 activators NCGC00186528 (TEPP-46) and NCGC00186527 (NCGC-527) were provided by the National Institutes of Health Chemical Genomics Center. Both compounds are from the thieno-[3,2-b]pyrrole[3,2-d]pyridazinone chemical class.[16]

Western blotting

Proteins from cell lysates were separated by sodium dodecyl sulfate polyacrylamide gel electrophoresis. Antibodies used included ALK (Invitrogen, Carlsbad, CA), *p*-ALK, PKM2, and pY105-PKM2 (Cell Signaling Technologies, Danvers, MA).

PKM2 activity

PKM2 activity assays were performed as previously described.[17]

Metabolic assays

Lactate and ATP were measured in conditioned media and cell lysates, respectively, by commercially available kits (BioVision, Milpitas, CA).

Proliferation and colony formation assays

Proliferation was determined by serial cell counting with Trypan blue. Colony formation assays were performed with Methocult H4230 per the manufacturer's instructions. Colonies were grown for 14 days before staining with *p*-iodonitrotetrazolium chloride (Sigma-Aldrich, St. Louis, MO).

Xenograft experiments

SCID-Biege mice (Charles River, Wilmington, MA) were injected with 6e6 cells in the subcutaneous flank (100 μL injection volume containing 50% Becton Dickenson Matrigel; BD, San Jose, CA). Tumors were measured with calipers and volumes were determined: $V = (0.5)(LW^2)$. Sample sizes of <6 were computed using a power of 0.8 from analogous experiments.[16]

All animal studies were performed under the compliance of University Committee on Use and Care of Animals protocol number PRO00003289.

Results

Phosphoproteomic analysis reveals NPM-ALK–mediated phosphorylation of metabolic proteins

We used a MS-based phosphoproteomic strategy to identify novel mediators of ALK signaling (Figure 1A) in ALCL-derived cells treated with a specific small molecule inhibitor of ALK (CEP-26939).[15] Six-hour exposure to CEP was long enough to observe complete abrogation of ALK autophosphorylation at Y1604-ALK in NPM-ALK$^+$ ALCL cell lines (SU-DHL-1 and SUPM2) but not long enough to significantly impact cell viability (supplemental Figure 1A-B).[15] Phosphoproteomic analysis of SU-DHL-1 revealed that ALK inhibition resulted in the down-regulation of 569 proteins and up-regulation of 102 proteins (Figure 1B). As expected, the phosphoprotein that changed with greatest significance was ALK (z-score = −6.0). We established a significance threshold of $|z| \geqslant 1$ for the identification of candidate mediators of ALK signaling because this represents the outer 6.6% of the entire data and includes known ALK substrates. Forty-nine proteins (43 less than z = −1 and 6 greater than z = 1) met this statistical criterion, including previously known ALK substrates signal transducer and activator of transcription 3 (z = −2.2) and Src homology 2 domain-containing transforming protein 1 (z = −3.6).[2,18]

To functionally categorize the phosphoprotein changes, we used the Database for Annotation, Visualization and Integrated Discovery[19,20] (Figure 1C-D). Gene Ontology (GO) biological process term analysis identified numerous processes that were regulated by ALK activity, including "transmembrane receptor tyrosine kinase (RTK) signaling pathway," "positive regulation of cell proliferation," and "metabolic process," among others (Figure 1C). Further analysis of the "metabolic process" GO term into its constituents revealed alterations of metabolic pathways such as "nucleotide metabolic process," "macromolecule metabolic process," "biosynthetic process," and "glycolysis" (Figure 1D). Supplemental Table 1 lists phosphoproteins clustered based on the Kyoto Encyclopedia of Genes and Genomes annotated metabolic pathways that were identified by phosphoproteomic analysis. Based on these results, we hypothesized that NPM-ALK regulates cellular metabolism via phosphorylation of proteins involved in key metabolic pathways including glycolysis, pentose phosphate, and the tricarboxylic acid (TCA) cycle.

Metabolomic analysis reveals NPM-ALK–mediated alterations in biomass-producing pathways

We carried out metabolomic profiling of SU-DHL-1 cells in the presence or absence of ALK activity (Figure 1A). As shown in Figure 2A, we observed large-scale and global changes in metabolites (mass spectral features) in response to ALK inhibition. Unsupervised hierarchical clustering of the 4784 mass spectral features revealed a high degree of reproducibility within the replicates and demonstrated a distinct metabolic signature associated with ALK activity (Figure 2A). Figure 2B depicts supervised clustering of mass spectral features that showed change of $P < .05$ (936 mass spectral features): 390 decreased and 546 increased in response to ALK inhibition.

We used MetaboAnalyst 2.0[21,22] to assess the metabolic pathways regulated by ALK. Figure 2C ranks the pathway results by *P* value, showing those pathways that were significantly altered by ALK signaling. The results showed significant changes in a number of pathways involved in biomass production, including purine, pyrimidine, glycerophospholipid and glycine, serine, and threonine metabolisms (all $P < .01$). Importantly, pathways affecting glycolysis, the pentose phosphate shunt, and the TCA cycle (all $P < .01$), which serve as the starting point for many biomass-producing pathways involved in the Warburg effect,[14] were also significantly altered by ALK. Supplemental Table 2 lists the metabolites that were regulated by ALK using a statistical cutoff of $P < .05$ based on 4 biological replicates. Quantities of metabolite levels were obtained from normalized area under the curve analysis from MS. Importantly, we identified changes in metabolites within the significant pathways highlighted by pathway analysis (Figure 2C).

Integrated analysis reveals NPM-ALK–regulated metabolic signature

We integrated the phosphoproteomic and metabolomic data sets to generate a global and unified view of the ALK-regulated metabolic signature. We used the Kyoto Encyclopedia of Genes and Genomes mapping tools to integrate our phosphoproteomic and metabolomic data sets into the human metabolic reference map (hsa01100).[23,24] As shown in Figure 3, each colored edge represents a metabolic reaction carried out by phosphoproteins (pY, pS, and pT) that was regulated by ALK. Each node represents a metabolite whose concentration was changed after ALK inhibition (green = down, red = up). There were

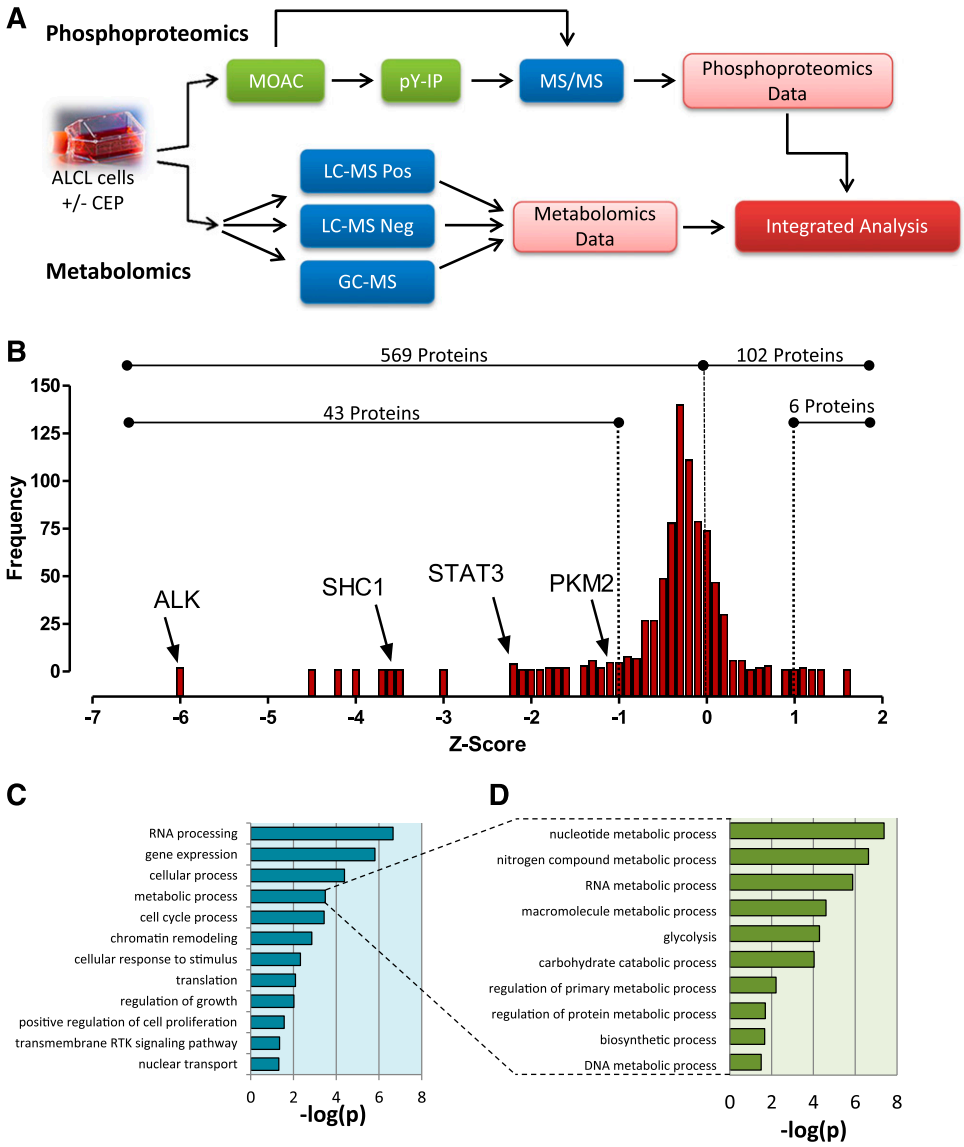

Figure 1. Phosphoproteomic analysis reveals NPM-ALK–mediated changes in metabolic pathways. (A) Experimental strategy used for phosphoproteomic and metabolomic analysis of ALK. NPM-ALK$^+$ cell lines were exposed to ALK inhibitor or DMSO. Phosphorylated peptides were enriched with metal oxide affinity chromatography (MOAC) followed by immunoprecipitation with pY antibodies and subjected to tandem MS analysis (biological triplicate). For the metabolomics, the cell lysates were subjected to LC-MS in both positive and negative mode, as well as gas chromatography MS (GC-MS). (B) The phosphoproteomic data plotted as number of proteins (frequency) vs the z-score based on change in spectral counts in response to ALK inhibition (CEP). A significance threshold was set at $|z| \geq 1$. (C) GO term enrichment analysis using Database for Annotation, Visualization and Integrated Discovery applied to the proteins that changed in spectral counts following ALK inhibiton. A subset of the significant terms is displayed and ranked by –log(p), the natural log of the *P* value. (D) List of GO terms that comprise the metabolic processes term.

concurrent changes in both metabolites and proteins in glycolysis, the TCA cycle, and nucleotide biosynthesis pathways. The significantly changed phosphoproteins and metabolites are shown in supplemental Tables 1 and 2, respectively. Specifically, both lactate (supplemental Table 1) and phosphorylated lactate dehydrogenase (supplemental Table 2) decreased in response to ALK inhibition. These data suggest that ALK regulates widespread changes in glycolysis, the pentose phosphate pathway, and pyrimidine metabolism by altering protein phosphorylation.

Metabolic flux analysis reveals NPM-ALK–regulated metabolic shift

Phosphoproteomic and metabolomic profiling highlighted global changes reflecting ALK-induced steady-state alterations in cellular metabolism. Specifically, the metabolomic analysis showed significant reduction in lactate (0.21 ± 0.056-fold [standard deviation (SD)], $P < .01$) following ALK inhibition (Figure 4A). To gain a better understanding of the kinetics of glucose metabolism, we determined the flux of glucose carbons through different metabolic pathways in ALCL-derived cells cultured in ^{13}C-glucose. [^{13}C]-isotopomers of various metabolites were determined by liquid chromatography-MS (LC-MS). After 30 minutes of growth in [U-^{13}C]-glucose, the majority of the lactate appeared as [m+3] (mass + 3 labeled carbons) demonstrating that it was derived directly from glucose (Figure 4B). ALK inhibition resulted in a significant reduction (0.52 ± 0.19-fold, $P < .05$) of glycolytic flux to lactate. The reduced flux to the lactate pool appears to be due to a reduced glucose uptake and glycolytic rate, because proximal glycolytic intermediates glucose-6-phosphate + fructose-6-phosphate and fructose-1,6-bisphosphate were significantly reduced (0.63-fold, $P < .01$ and 0.79-fold, $P < .05$, respectively; Figure 4C). Finally, ribose-5-phosphate/xylose-5-phosphate, which are key metabolites within the pentose phosphate shunt and support nucleotide biosynthesis, also showed a significant reduction of m + 5 labeling after ALK inhibition (0.61-fold, $P < .01$). Additionally, ALK inhibition induced a 2.33-fold increase (±0.33 SD, $P < .01$) in total pool ATP levels while reducing ADP levels to 0.28-fold of control (±0.054 SD, $P < .01$; Figure 4D). These data suggest that ALK activity results in a metabolic shift away from energy production favoring biomass production. Importantly, ATP levels are often used as a surrogate for cell health and viability,[25]

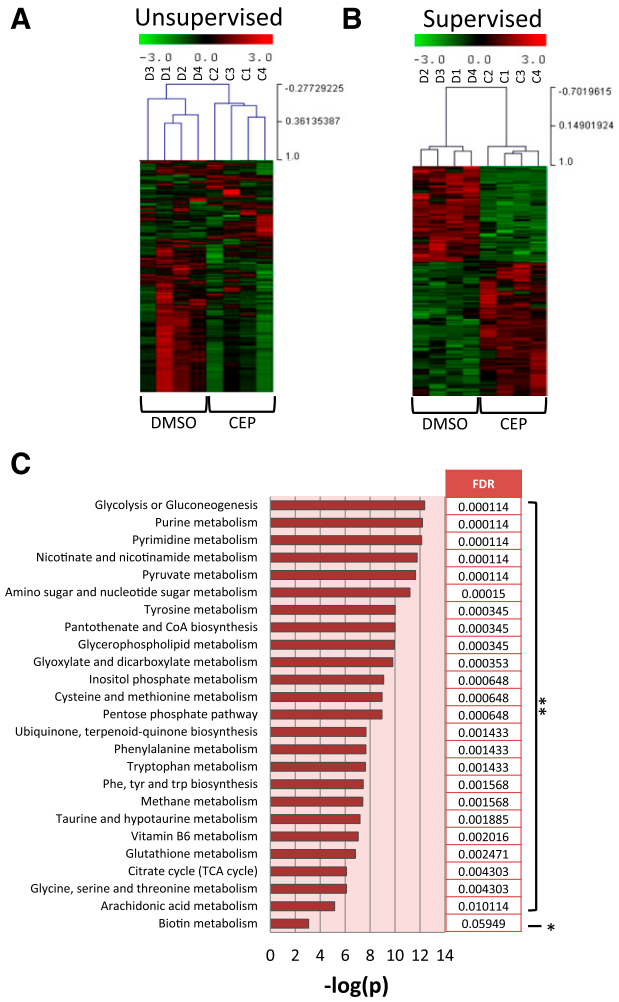

Figure 2. Metabolomic analysis reveals widespread metabolic changes driven by NPM-ALK signaling. (A) Unsupervised hierarchical clustering of all identified mass spectral features in DMSO- and CEP-treated cells (D1-D4 are DMSO samples; C1-C4 are CEP samples). (B) Supervised hierarchical clustering of those mass spectral features that changed significantly ($P < .05$) based on CEP treatment. (C) MetaboAnalyst 2.0–generated pathways that changed in response to ALK inhibition. *$P < .05$, **$P < .01$.

suggesting the decrease in glycolytic flux in response to ALK inhibition is not attributable to loss in cell viability.

To quantify the metabolic reprogramming for subsequent studies, we measured ATP and lactate levels using biochemical assays. Lactate is commonly used as a marker for aerobic glycolysis, which is necessary for biomass production.[14] A significant decrease in lactate was detected after ALK inhibition in 2 ALCL-derived cell lines (0.82 ± 0.026-fold [SD], $P < .01$ in DEL and 0.65 ± 0.029-fold [SD], $P < .01$ in SU-DHL-1) that correlated with an increase in ATP levels (1.15 ± 0.043-fold [SD], $P < .05$ in DEL and 1.48 ± 0.059-fold [SD], $P < .01$ in SU-DHL-1). No changes in lactate or ATP levels were observed in Jurkat cells (ALK negative; Figure 4E). These data highlight a metabolic shift driven by ALK to increase biomass production and a decrease energy production.

PKM2 is a substrate of NPM-ALK

PKM2 is a tumor-specific isoform of PK and a key regulator of glucose metabolism.[26] Based on the integrated proteomic/metabolomic analysis, we pursued the hypothesis that ALK-directed changes in cellular metabolism were mediated through phosphorylation of PKM2. Our phosphoproteomic analysis identified a significant reduction in phospho-PKM2 following ALK inhibition ($z = -1.1$; Figure 1B). The MS data showed 2 unique tyrosine phosphorylated peptides of PKM2 (containing Y105 and Y390; supplemental Figure 1C-D). Figure 5A tabulates the spectral counts of ALK and PKM2 that were determined in a representative experiment on SU-DHL-1 cells. There was a significant reduction of spectral counts of ALK-derived phospho-Tyr peptides (76 in dimethyl sulfoxide [DMSO] to 0 in CEP) and a reduction in pY105-PKM2 from 9 (DMSO) to 2 (CEP).

Additionally, we studied 9 T/NK lymphoma-derived cell lines using phosphoproteomic analysis (supplemental Figure 2A). Phosphorylated peptides derived from PKM2 were identified in all 4 of the ALK^+ ALCL cell lines, as well as the natural killer/T-cell lymphomas but not in the ALK^- ALCL, Sézary syndrome, and mycosis fungoides cells. Western blot analysis corroborated these findings, showing the levels of pY105-PKM2 were highest in the ALK^+ ALCL cells (SU-DHL-1, SUPM2, Karpas299) and the YT cells (supplemental Figure 2B), whereas the rest of the cell lines expressed negligible levels. There was little difference in the expression of total PKM2. These data provided the rationale to pursue subsequent studies characterizing PKM2 as a mediator of ALK-regulated metabolic switch.

Western blot analysis revealed that inhibition of ALK resulted in a marked reduction of pY105 PKM2 (56% of control) without a change in total PKM2 (Figure 5B). We observed similar results using another specific inhibitor of ALK (Crizotinib)[27] in 2 additional ALCL-derived cell lines. Crizotinib treatment led to a significant decrease in pY105-PKM2 in a dose-dependent manner (62% and 15% in SUPM2 and DEL, respectively, with 300 nM; supplemental Figure 2C). Transfection of 293T cells with wild-type (WT) NPM-ALK resulted in an increase in pY105-PKM2 (152%) compared with kinase-deficient mutant K210R NPM-ALK (Figure 5C). These results suggest that NPM-ALK regulates the phosphorylation of Y105-PKM2.

To determine whether PKM2 is a direct substrate of ALK kinase activity, we carried out in vitro kinase assays using immunoaffinity-purified WT or K210R GFP-NPM-ALK and His-tagged WT, Y105F, or Y390F PKM2 purified from *Escherichia coli* and incubated with ATP prior to western blotting. As shown in Figure 5D, WT NPM-ALK was autophosphorylated, whereas the K210R NPM-ALK mutant was not. WT PKM2 was phosphorylated at the Y105 residue in the presence of active NPM-ALK but not in the presence of K210R NPM-ALK. Furthermore, pY105-PKM2 was not detected in the presence of Y105F-PKM2. The Y390F-PKM2 mutant was also phosphorylated at the Y105 residue by WT NPM-ALK. These data show that ALK directly phosphorylates Y105-PKM2.

NPM-ALK regulates PKM2 activity via Y105 phosphorylation

We next sought to determine the effect of ALK-mediated phosphorylation of PKM2 on its enzymatic activity using a previously described assay.[17] As shown in Figure 5E, ALK inhibition resulted in a significant increase in PKM2 activity (1.59-fold, $P < .01$). Similarly, 293T cells transfected with WT NPM-ALK showed a reduction of PKM2 activity to 0.86-fold (±0.029 SD) compared with mock-transfected cells and the K210R NPM-ALK mutant (Figure 5F). To directly evaluate the function of pY105-PKM2, we generated cell lines stably expressing the Y105F-PKM2 mutation (Figure 5G). As shown in Figure 5H, DEL cells expressing Y105F-PKM2 displayed a 1.68-fold (±0.06 SD) increase in PKM2 activity compared with WT-PKM2. These data demonstrate that ALK phosphorylates PKM2, resulting in inhibition of its enzymatic activity.

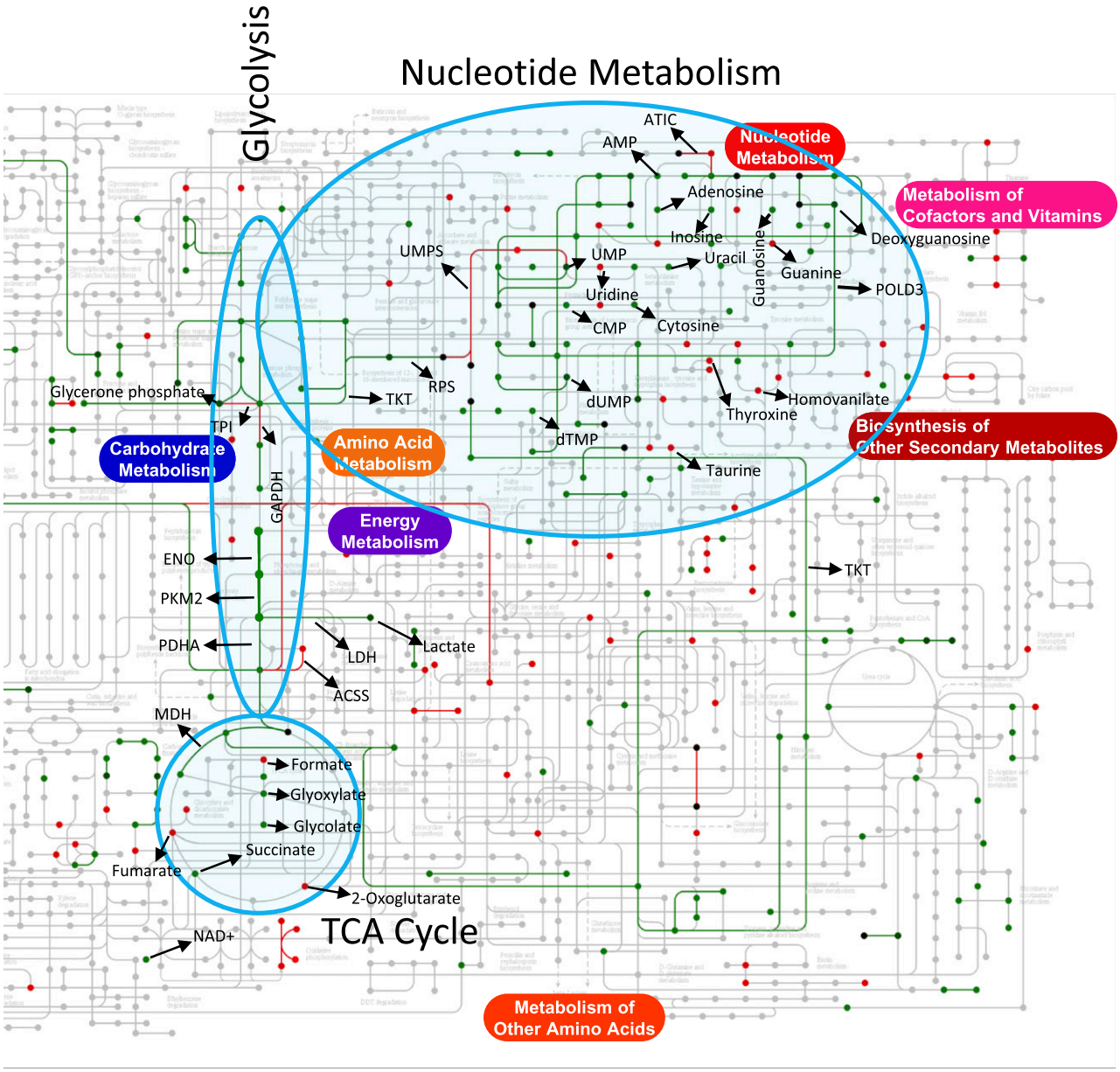

Figure 3. Integrated "omic" analysis reveals global metabolic changes. Kyoto Encyclopedia of Genes and Genomes "search&color pathway" analysis for phosphoproteins and metabolites overlaid on the human metabolic reference map (hsa01100). Phosphoproteomic data from one biological replicate of the SU-DHL-1 were used, whereas metabolomic data from 4 averaged biological replicates of SU-DHL-1 cells were used. Metabolites that changed (Student *t* test, $P < .05$) in response to CEP treatment were used. Green and red represent decrease and increase, respectively. Lines represent phosphoprotein and dots represent metabolites. Blue shading over glycolysis, TCA cycle, and nucleotide metabolism serve to highlight pathways that are highly represented.

Phosphorylation of PKM2 alters cellular metabolism

To assess the biological implications of the ALK-PKM2 axis, we evaluated the effect of 2 small molecule activators of PKM2 on cellular metabolism. The 2 compounds (TEPP-46 and NCGC-527) were derived from the same chemical class and differ only by 1 side-group.[16] Treatment of SU-DHL-1 and DEL cells with the 2 activators caused a significant increase in PKM2 activity (Figure 6A). The activation of PKM2 triggered a significant decrease in lactate production (0.8 ± 0.064-fold [SD], $P < .01$ in Karpas299 cells and 0.77 ± 0.05-fold [SD], $P < .01$ in DEL cells; Figure 6B). An increase in ATP levels was also observed (1.67 ± 0.12-fold [SD], $P < .01$ in Karpas299 and 1.19 ± 0.01-fold [SD], $P < .01$ in DEL). Jurkat cells did not show a significant change in lactate or ATP levels following PKM2 activation by either compound. Similarly, DEL cells expressing Y105F-PKM2 also exhibited a metabolic shift compared with WT-PKM2–expressing cells (0.58 ±0.077-fold [SD], $P < .01$ less lactate and 1.69 ± 0.032-fold [SD], $P < .01$ more ATP; Figure 6C). These data indicate that phosphorylation of PKM2 by NPM-ALK leads to inhibition of its activity and altered cellular metabolism.

Phosphorylation of PKM2 regulates cell proliferation

Next, we investigated the effect of PKM2 phosphorylation on cell proliferation. DEL cells were treated with increasing concentrations of PKM2 activator (NCGC-527), and cell proliferation was monitored over 72 hours by cell counting with Trypan blue stain

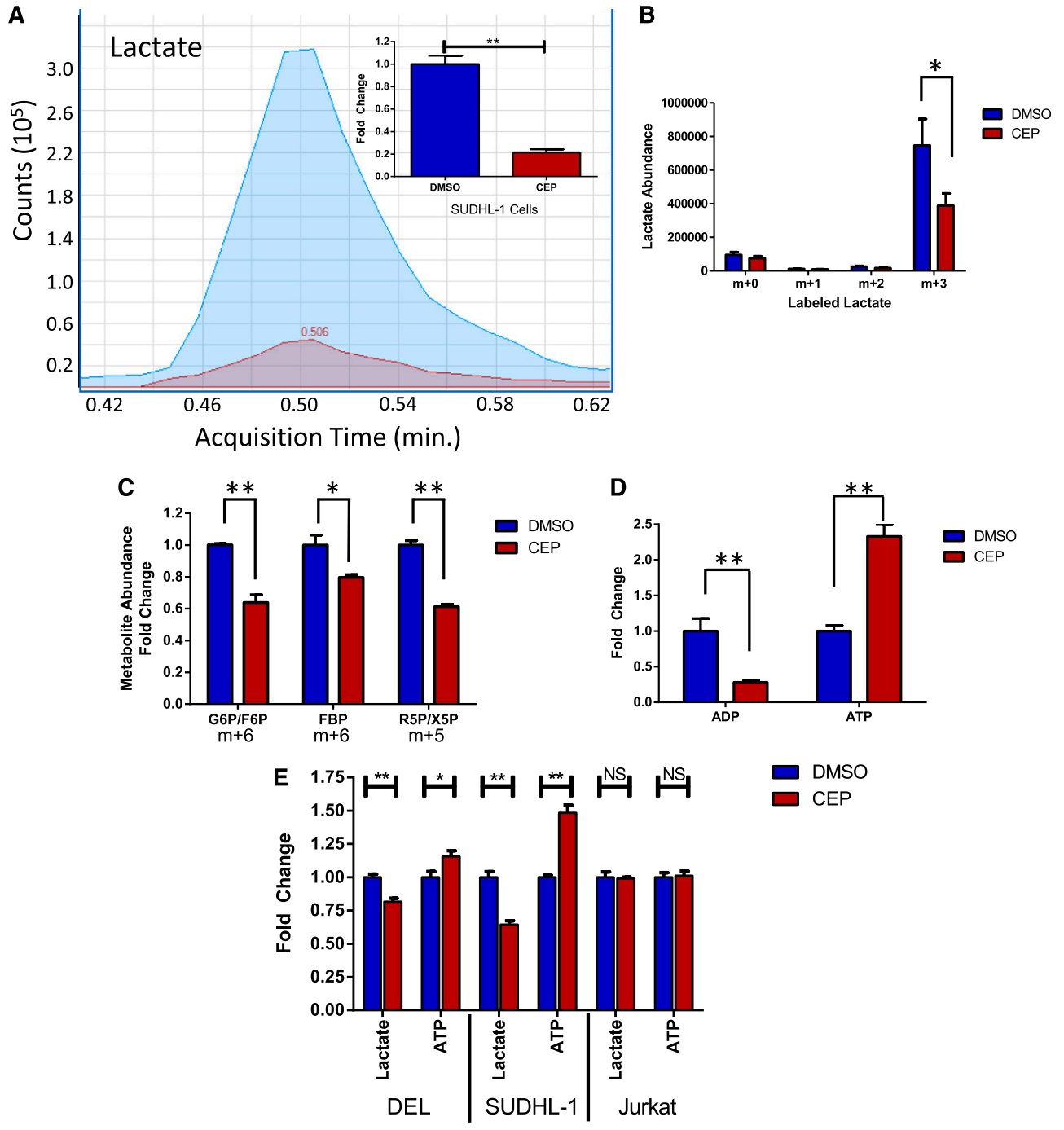

Figure 4. Metabolic flux analysis reveals NPM-ALK–driven shift toward biomass production. (A) Quantitation of lactate levels by metabolomic analysis. Representative spectra for DMSO- (blue) and CEP- (red) treated cells. The quantitation of lactate based on 4 replicates is shown in the inset. (B) Metabolic flux analysis of lactate in SU-DHL-1 cell following 300 nM CEP treatment. All species of labeled lactate are shown. m, mass. (C) Flux analysis for fully labeled glucose 6-phosphate/fructose 6-phosphate (G6P/F6P), fructose bisphosphate (FBP), and ribose 5-phosphate/xylose 5-phosphate (R5P/X5P) are shown in the presence of DMSO or ALK inhibitor. (D) Total pool abundance (all labeled and unlabeled species combined) for ADP and ATP in the presence of DMSO or ALK inhibitor. (E) Biochemical assays for lactate and ATP after 300 nM CEP for 6 hours. Data are normalized by cell number. Mean ± SD; *$P < .05$, **$P < .01$.

under normoxic (21% O_2) and hypoxic (3% O_2) conditions. A dose-dependent reduction in proliferation was observed throughout 72-hour exposure to NCGC-527 (30 μM), showing a 54% (±8.6% [SD], $P < .01$) reduction under normoxia and a 69% (±5% [SD], $P < .01$) reduction in hypoxia (Figure 6D). Interestingly, under normoxic conditions, cultures still maintained >85% viability (Trypan blue staining) under the highest concentration of NCGC-527, whereas cells exposed to hypoxic conditions demonstrated a dose-dependent decrease in cell viability (49 ± 11% [SD], $P < .01$, viability after 72 hours; Figure 6E). These data suggest that chemical activation of PKM2 results in a metabolic shift from anaerobic glycolysis to oxidative phosphorylation.

Similarly, when DEL cells were exposed to both the PKM2 activator and oligomycin (ATP synthase inhibitor)[28] under normoxia, an additive reduction of cell proliferation was observed (39± 4.7% [SD], $P < .01$, compared with DMSO control;

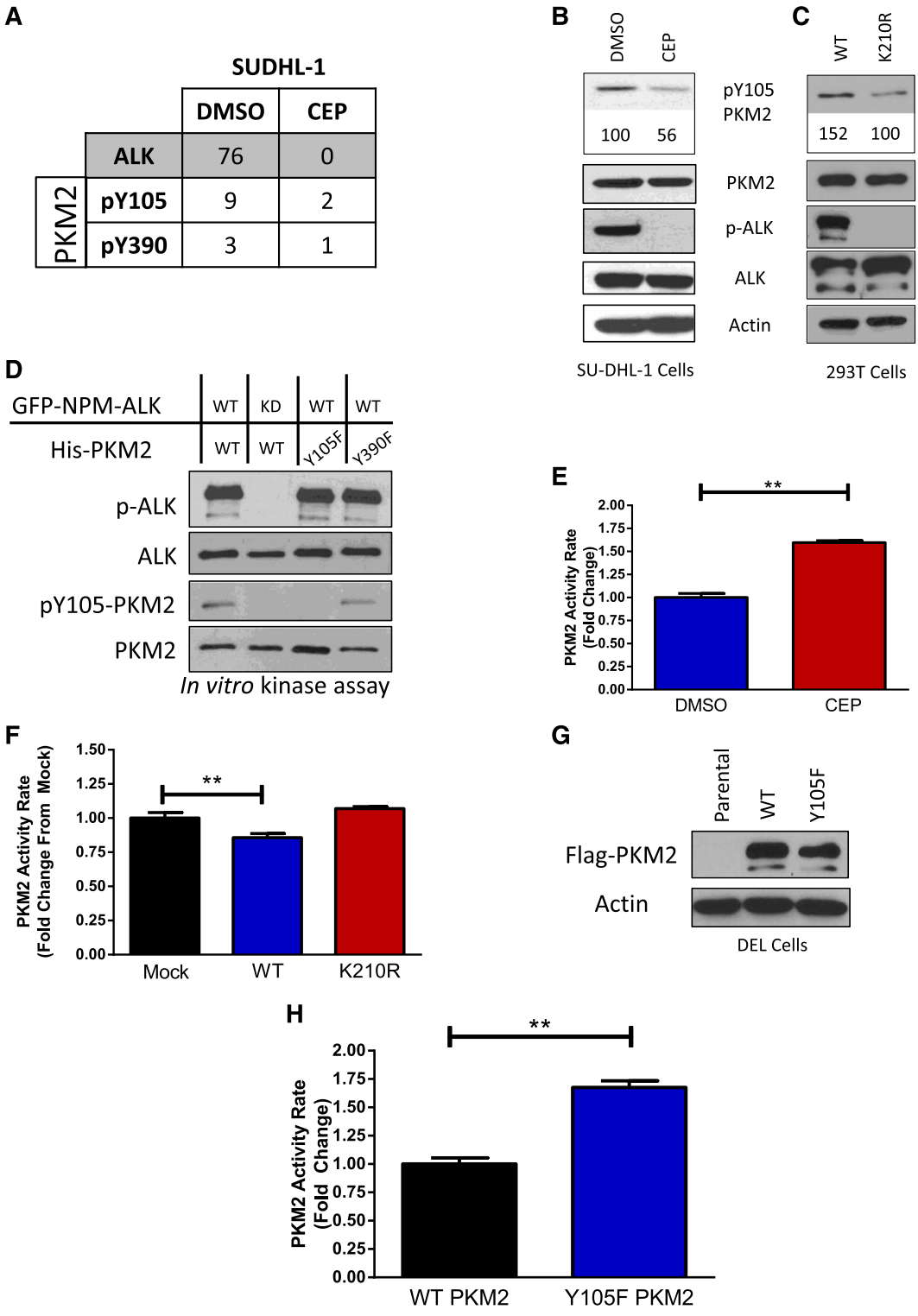

Figure 5. NPM-ALK regulates the phosphorylation and activity of PKM2. (A) Changes in *p*-ALK and *p*-PKM2 in response to ALK inhibition. The spectral counts for ALK (all phosphorylated peptides) and the 2 identified PKM2 phosphopeptides are shown. (B) Immunoblots of lysates from SU-DHL-1 cells following CEP treatment of 6 hours at 300 nM CEP. (C) Immunoblots of 293T lysates that were transiently transfected with either WT NPM-ALK or K210R NPM-ALK. (D) In vitro kinase assay with purified His-PKM2 (WT, Y105F, or Y390F) and ALK immunoprecipitation using GFP-NPM-ALK (WT or K210R). (E) PKM2 activity assay for SUPM2 cells treated with 100 nM CEP for 4 hours. (F) PKM2 activity assay on lysates from 293T cells transfected with mock, WT NPM-ALK, or K210R NPM-ALK. (G) Stable expression of Flag-PKM2 in DEL cells. (H) PKM2 activity assay of DEL cells stably expressing WT or Y105F PKM2. Data are mean ± SD; $^{**}P < .01$.

Figure 6F). Furthermore, DEL cells expressing Y105F-PKM2 were more sensitive to oligomycin (72 hours) and resulted in a 30% (±12% [SD], $P < .05$) reduction in cell number relative to DMSO control, whereas oligomycin had a minimal effect (91 ± 11% of control [SD], $P = .2$) in DEL cells expressing WT-PKM2 (Figure 6G). The increased sensitivity of Y105F-PKM2–expressing cells to ATP synthase inhibition suggests that they were more reliant on oxidative phosphorylation than their WT counterpart.

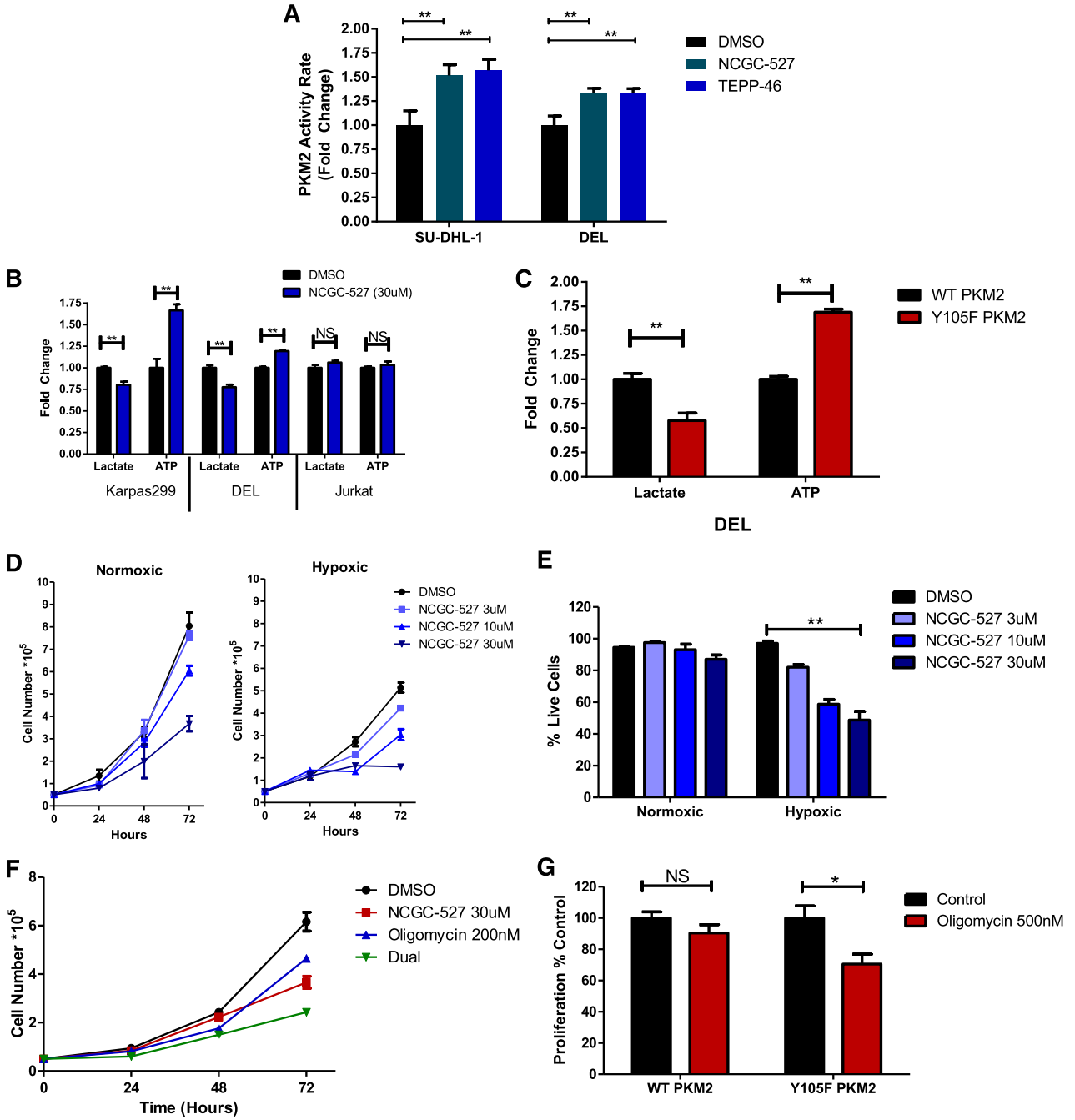

Figure 6. PKM2 regulates metabolic switch and proliferation. (A) PKM2 activity assay using SU-DHL-1 treated with 10 μM NCGC-527 for 24 hours. (B) Lactate and ATP assays using conditioned media and cell lysates (respectively) on Karpas299, DEL, and Jurkat cells following 6-hour treatment with 30 μM NCGC-527. (C) Lactate and ATP assays of DEL cells stably expressing Flag-PKM2 WT of Flag-PKM2 Y105F. (D) Cellular proliferation measured by serial counting with Trypan blue stain of DEL cells treated with indicated concentrations of NCGC-527. Cells were maintained in either normoxic or hypoxic (3% O_2) conditions. (E) Viability data from D showing the percentage live cells under the indicated conditions. (F) Cell proliferation of DEL cells treated with NCGC-527, oligomycin, or both. (G) Cell proliferation of DEL cells stably expressing Flag-PKM2 and treated with DMSO or 500 nM oligomycin for 72 hours. Counts were normalized to each control (DMSO) condition. Data are mean ± SD; $^*P < .05$, $^{**}P < .01$, not significant (NS).

These data support the role for phosphorylation and inhibition of PKM2 as a key regulatory mechanism for the metabolic switch toward anaerobic glycolysis and consequent impact on cell proliferation.

PKM2 regulates tumorigenesis

To investigate the role of PKM2 in tumorigenesis of ALK^+ ALCL, methylcellulose colony formation assays were conducted. Activation of PKM2 caused a significant reduction of colonies in a dose-dependent manner (39± 2.2% [SD], $P < .01$, with 30 μM NCGC-527; Figure 7A). Furthermore, DEL cells expressing Y105F-PKM2 showed significantly reduced colony numbers compared with WT-PKM2 (54 ± 7.9% [SD], $P < .05$; Figure 7B). These data indicate that the activity and phosphorylation of PKM2 contribute to the tumorigenic potential of ALK^+ ALCL cells in vitro.

To determine the role of PKM2 in ALK^+ ALCL tumorigenesis in vivo, we evaluated the PKM2 activators and Y105F-PKM2 in xenografted tumors in mice. TEPP-46 was used for this study based on the availability of the compound and the similarity of the

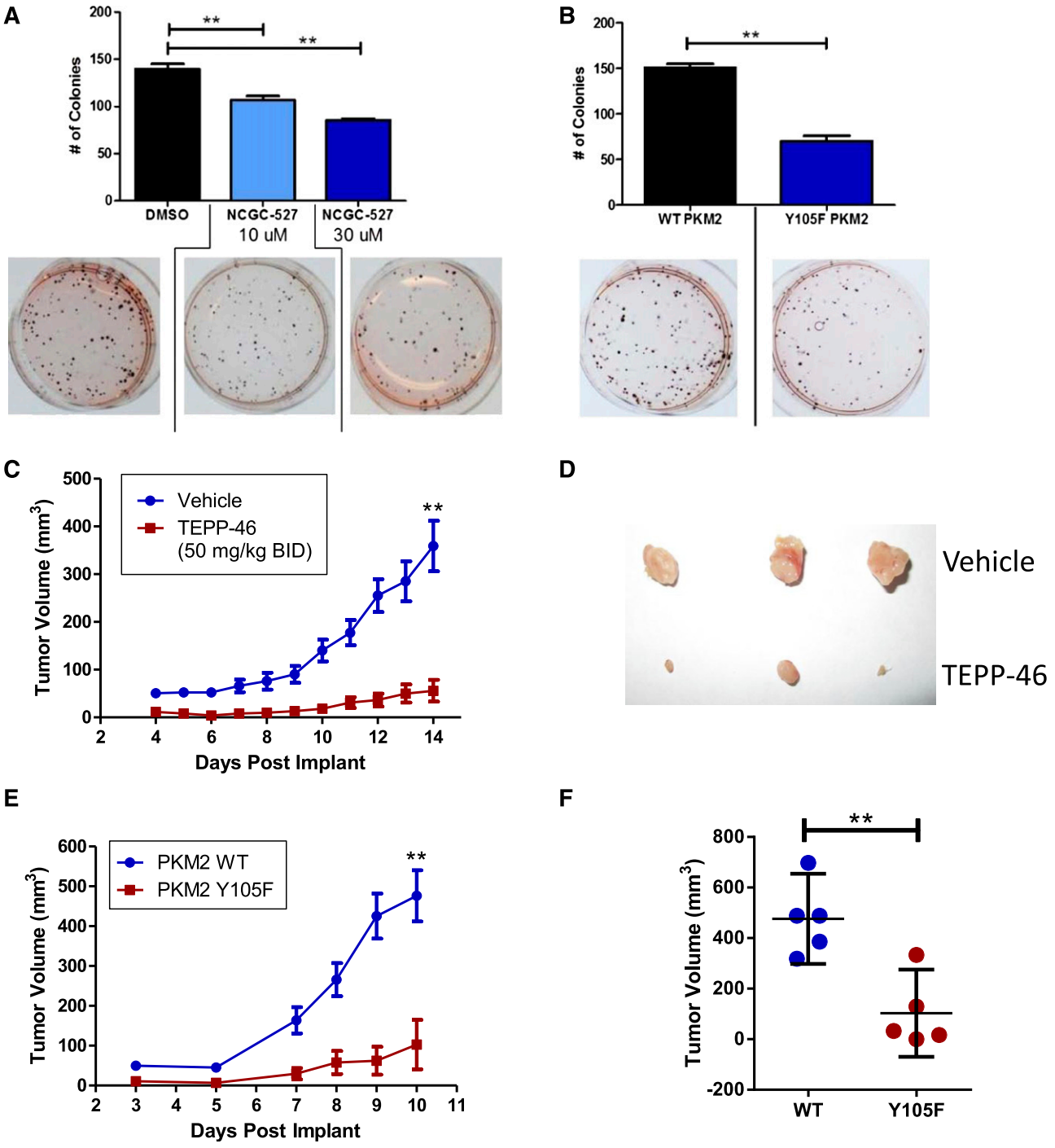

Figure 7. PKM2 regulates ALCL tumorigenesis. Methylcellulose colony formation assay using (A) DEL cells treated with 10 and 30 μM NCGC-527 and (B) DEL cells stably expressing Flag-PKM2 WT and Y105F. Samples analyzed in triplicate, with a representative image shown below each bar. Data are mean ± SD. (C) Tumor volumes of DEL xenograft tumors treated with vehicle (0.5% methylcellulose + 0.1% Tween 80) or TEPP-46 (50 mg/kg) twice a day by oral dose from day of tumor implantation (mean ± SEM) (n = 7). (D) Representative images of tumors at day 14. (E) Tumor volumes of xenografted DEL cells stably expressing WT or Y105F-PKM2 (mean ± SEM; n = 5). (F) Scatterplot of day 10 tumor volumes. Data are mean ± 95% confidence interval; *$P < .05$, **$P < .01$.

in vitro effects on PKM2 activity and cell proliferation with NCGC-527 (Figure 6A; data not shown). SCID-Beige mice (n = 7) were subcutaneously implanted with DEL cells and dosed with either vehicle or TEPP-46 on the day of tumor injection. As shown in Figure 7C, 14 days after implantation, the vehicle-treated mice showed significant tumor growth (359 ± 63 mm^3 [standard error of the mean (SEM)]), whereas the TEPP-46–treated mice showed marked retardation in tumor growth, with a mean tumor volume of 56 mm^3 (±27 mm^3 [SEM], $P < .01$; 3/7 mice developed no measurable tumors). Figure 7D shows the gross images of 3 representative tumors from vehicle-treated (upper) and TEPP-46–treated mice (lower).

DEL cells stably expressing WT or Y105F PKM2 were implanted in SCID-Beige mice (n = 5), and tumor volumes were measured over 10 days (Figure 7E). Mice xenografted with cells expressing Y105F-PKM2 showed significant reduction in tumor volume compared with

WT (103 vs 476 mm^3, $P < .01$; Figure 7F). Western blot analysis was performed to assess the level of exogenous Flag-PKM2 expressed in the injected cells compared with the resulting tumors. Interestingly, excised Y105F-PKM2 tumors lost expression of the mutant gene compared with injected cells, whereas WT-PKM2 tumors did not (supplemental Figure 2D). Importantly, the 2 Y105F-PKM2 tumors shown in supplemental Figure 2D were the only tumors in this group that were large enough to produce protein extracts. These data support the conclusion that the Y105F-PKM2 expression is detrimental to tumor growth, in agreement with that previously reported.[16] Taken together, these data indicate that the phosphorylation and inhibition of PKM2 is an important aspect of ALK-regulated tumorigenesis in ALCL.

Discussion

Integrated analysis of the phosphoproteomic, metabolomic, and metabolic flux data identified a novel role of ALK in the regulation of cellular metabolism. Proteins and metabolites within glycolysis, the pentose phosphate shunt, and pyrimidine metabolic pathways were significantly regulated by the tyrosine kinase activity of ALK. The observations indicate that oncogenic signaling of ALK results in an increase in biomass production by rerouting glycolytic intermediates. The integrated analysis rationalized the hypothesis that ALK phosphorylates PKM2, a key enzyme in glycolysis, thereby resulting in a metabolic switch to promote tumorigenesis.

PKM2 is a key regulator of aerobic glycolysis and is frequently expressed in tumors and proliferating cells.[26] The enzymatic activity of PKM2 has been shown to be regulated by tyrosine phosphorylation and phosphorylated peptide binding,[17,29] with consequent diversion of glycolytic intermediates toward biomass production. Our data provide evidence that phosphorylation of Y105-PKM2 by ALK represents a mechanism by which lymphoma cells acquire a metabolic advantage facilitating tumor growth. Pharmacological activation of PKM2 and the expression of Y105F-PKM2 were effective in reversing the metabolic switch and subsequent proliferation and tumorigenesis. Our data substantiate the role of PKM2 in metabolic reprogramming in lymphoid cells and expands the spectrum of oncogenic kinases that regulates its activity. The generation of $CD4^+$ T-cell conditional PKM knockout mice may yield further insight into the tumorigenic capacity of PKM2 and warrant further study.

Phosphoproteomic and metabolomic analysis also indicated that lipid metabolism, amino acid metabolism, and nucleotide metabolism were regulated by ALK (supplemental Tables 1 and 2). Phosphorylation or transcriptional regulation of metabolic enzymes involved in these pathways, such as lactate dehydrogenase A,[30,31] mitochondrial pyruvate dehydrogenase kinase 1,[32] and phosphoglycerate mutase 1,[33] have been implicated in mediating an oncogenic metabolic switch. Recent studies highlighting the importance of citrate metabolism or impaired TCA cycle function in cancer cells support the notion that metabolic adaption is a hallmark of oncogenesis.[34] We also identified significant changes in glycine, serine, and threonine metabolism in response to ALK inhibition (Figure 2C). Recent studies have demonstrated that PKM2 may regulate de novo serine synthesis from the glycolytic intermediate 3-phosphoglycerate.[35,36] The amino acid serine contributes to increased cellular biomass and the activation of mammalian target of rapamycin complex 1 (mTORC1).[35] Given the previously demonstrated effect of ALK in the activation of mTORC1,[37] our results provide a potential link between ALK and serine synthesis through PKM2. Accordingly, future studies to elucidate the molecular mechanisms underlying ALK-dependent regulation of proteins and metabolites within lipid metabolism, nucleotide synthesis, and amino acid metabolism are warranted.

Our findings suggest that PKM2 may serve as a therapeutic target in ALCL. Although most patients respond well to aggressive chemotherapeutic agents, many patients experience relapses and recurrence.[38] Recently developed small molecule inhibitors of ALK show promising early responses in NPM-ALK^+ ALCL. However, a subset develops resistance, highlighting the need to expand on therapeutic options.[39] The ability of PKM2 activators to reduce tumor engraftment and slow tumor growth suggests these agents may be effective in combination with other cytotoxic therapies. Combination therapies that target multiple signaling pathways including ALK-mediated metabolic changes may provide additional benefit and are worth investigating in clinical trial settings. Additionally, this work opens the possibility that similar metabolic reprogramming mechanisms may be present in other types of lymphoma (specifically natural killer/T-cell lymphomas). Further exploration into this hypothesis and the potential therapeutic advantages in these tumors is warranted.

Acknowledgments

This work was supported by the Michigan Regional Comprehensive Metabolomics Resource Core (1U24 DK097153), National Institutes of Health, National Cancer Institute grants R01 CA140806-01 (to M.S.L), R01 DE119249, R01 CA136905 (to K.S.J.E.-J.), 5T32 GM070449 (to T.W.), and 1F31 CA171373-01 (to S.R.P.M.), and the A. Alfred Taubman Institute (to C.F.B.).

Authorship

Contribution: S.R.P.M. prepared the manuscript and designed and conducted experiments; S.R.H. conducted experiments; D.R., V.B., and K.P.C. performed phosphoproteomic MS analysis; D.F., T.W., and A.R. carried out informatics analysis; C.M.-Z. generated stable cell lines; C.R. and C.F.B. performed metabolomic analysis; J.-K.J. and C.J.T. generated and scaled PKM2 activating compounds; C.M.H. directed animal studies; and K.S.J.E.-J. and M.S.L. designed experiments and prepared the manuscript.

Conflict-of-interest disclosure: The authors declare no competing financial interests.

Correspondence: Megan S. Lim, Biomedical Science Research Building, Room 2039, 109 Zina Pitcher Place, Ann Arbor, MI 48109; e-mail: meganlim@med.umich.edu.

References

1. Amin HM, Lai R. Pathobiology of ALK+ anaplastic large-cell lymphoma. *Blood.* 2007;110(7):2259-2267.
2. Bischof D, Pulford K, Mason DY, Morris SW. Role of the nucleophosmin (NPM) portion of the non-Hodgkin's lymphoma-associated NPM-anaplastic lymphoma kinase fusion protein in oncogenesis. *Mol Cell Biol.* 1997;17(4):2312-2325.
3. Soda M, Choi YL, Enomoto M, et al. Identification of the transforming EML4-ALK fusion gene in non-small-cell lung cancer. *Nature.* 2007;448(7153):561-566.
4. Janoueix-Lerosey I, Lequin D, Brugières L, et al. Somatic and germline activating mutations of the ALK kinase receptor in neuroblastoma. *Nature.* 2008;455(7215):967-970.
5. Griffin CA, Hawkins AL, Dvorak C, Henkle C, Ellingham T, Perlman EJ. Recurrent involvement

of 2p23 in inflammatory myofibroblastic tumors. *Cancer Res.* 1999;59(12):2776-2780.

6. Amin HM, McDonnell TJ, Ma Y, et al. Selective inhibition of STAT3 induces apoptosis and G(1) cell cycle arrest in ALK-positive anaplastic large cell lymphoma. *Oncogene.* 2004;23(32): 5426-5434.
7. Bai RY, Dieter P, Peschel C, Morris SW, Duyster J. Nucleophosmin-anaplastic lymphoma kinase of large-cell anaplastic lymphoma is a constitutively active tyrosine kinase that utilizes phospholipase C-γ to mediate its mitogenicity. *Mol Cell Biol.* 1998;18(12):6951-6961.
8. Crockett DK, Lin Z, Elenitoba-Johnson KS, Lim MS. Identification of NPM-ALK interacting proteins by tandem mass spectrometry. *Oncogene.* 2004;23(15):2617-2629.
9. Slupianek A, Nieborowska-Skorska M, Hoser G, et al. Role of phosphatidylinositol 3-kinase-Akt pathway in nucleophosmin/anaplastic lymphoma kinase-mediated lymphomagenesis. *Cancer Res.* 2001;61(5):2194-2199.
10. McDonnell SRP, Hwang SR, Basrur V, et al. NPM-ALK signals through glycogen synthase kinase 3β to promote oncogenesis. *Oncogene.* 2012;31(32):3733-3740.
11. Lim MS, Carlson ML, Crockett DK, et al. The proteomic signature of NPM/ALK reveals deregulation of multiple cellular pathways. *Blood.* 2009;114(8):1585-1595.
12. Hanahan D, Weinberg RA. Hallmarks of cancer: the next generation. *Cell.* 2011;144(5):646-674.
13. Warburg O, Wind F, Negelein E. The metabolism of tumors in the body. *J Gen Physiol.* 1927;8(6): 519-530.
14. Lunt SY, Vander Heiden MG. Aerobic glycolysis: meeting the metabolic requirements of cell proliferation. *Annu Rev Cell Dev Biol.* 2011;27: 441-464.
15. Ott GR, Tripathy R, Cheng M, et al. Discovery of a potent Inhibitor of anaplastic lymphoma kinase with in vivo antitumor activity. *ACS Med Chem Lett.* 2010;1(9):493-498.
16. Anastasiou D, Yu Y, Israelsen WJ, et al. Pyruvate kinase M2 activators promote tetramer formation and suppress tumorigenesis. *Nat Chem Biol.* 2012;8(10):839-847.
17. Hitosugi T, Kang S, Vander Heiden MG, et al. Tyrosine phosphorylation inhibits PKM2 to promote the Warburg effect and tumor growth. *Sci Signal.* 2009;2(97):ra73.
18. Chiarle R, Simmons WJ, Cai H, et al. Stat3 is required for ALK-mediated lymphomagenesis and provides a possible therapeutic target. *Nat Med.* 2005;11(6):623-629.
19. Huang W, Sherman BT, Lempicki RA. Bioinformatics enrichment tools: paths toward the comprehensive functional analysis of large gene lists. *Nucleic Acids Res.* 2009;37(1):1-13.
20. Huang W, Sherman BT, Lempicki RA. Systematic and integrative analysis of large gene lists using DAVID bioinformatics resources. *Nat Protoc.* 2009;4(1):44-57.
21. Xia J, Mandal R, Sinelnikov IV, Broadhurst D, Wishart DS. MetaboAnalyst 2.0—a comprehensive server for metabolomic data analysis. *Nucleic Acids Res.* 2012;40(Web Server issue):W127-W133.
22. Xia J, Psychogios N, Young N, Wishart DS. MetaboAnalyst: a web server for metabolomic data analysis and interpretation. *Nucleic Acids Res.* 2009;37(Web Server issue):W652-W660.
23. Kanehisa M, Goto S, Sato Y, Furumichi M, Tanabe M. KEGG for integration and interpretation of large-scale molecular data sets. *Nucleic Acids Res.* 2012;40(Database issue): D109-D114.
24. Ogata H, Goto S, Sato K, Fujibuchi W, Bono H, Kanehisa M. KEGG: Kyoto Encyclopedia of Genes and Genomes. *Nucleic Acids Res.* 1999; 27(1):29-34.
25. Maehara Y, Anai H, Tamada R, Sugimachi K. The ATP assay is more sensitive than the succinate dehydrogenase inhibition test for predicting cell viability. *Eur J Cancer Clin Oncol.* 1987;23(3): 273-276.
26. Christofk HR, Vander Heiden MG, Harris MH, et al. The M2 splice isoform of pyruvate kinase is important for cancer metabolism and tumour growth. *Nature.* 2008;452(7184):230-233.
27. Christensen JG, Zou HY, Arango ME, et al. Cytoreductive antitumor activity of PF-2341066, a novel inhibitor of anaplastic lymphoma kinase and c-Met, in experimental models of anaplastic large-cell lymphoma. *Mol Cancer Ther.* 2007; 6(12 Pt 1):3314-3322.
28. Lardy HA, Connelly JL, Johnson D. Antibiotics as tools for metabolic studies. II. Inhibition of phosphoryl transfer in mitochondria by oligomycin and aurovertin. *Biochemistry.* 1964;3(12): 1961-1968.
29. Christofk HR, Vander Heiden MG, Wu N, Asara JM, Cantley LC. Pyruvate kinase M2 is a phosphotyrosine-binding protein. *Nature.* 2008; 452(7184):181-186.
30. Shim H, Dolde C, Lewis BC, et al. c-Myc transactivation of LDH-A: implications for tumor metabolism and growth. *Proc Natl Acad Sci USA.* 1997;94(13):6658-6663.
31. Fan J, Hitosugi T, Chung TW, et al. Tyrosine phosphorylation of lactate dehydrogenase A is important for NADH/NAD(+) redox homeostasis in cancer cells. *Mol Cell Biol.* 2011;31(24): 4938-4950.
32. Hitosugi T, Fan J, Chung TW, et al. Tyrosine phosphorylation of mitochondrial pyruvate dehydrogenase kinase 1 is important for cancer metabolism. *Mol Cell.* 2011;44(6):864-877.
33. Hitosugi T, Zhou L, Elf S, et al. Phosphoglycerate mutase 1 coordinates glycolysis and biosynthesis to promote tumor growth. *Cancer Cell.* 2012; 22(5):585-600.
34. DeBerardinis RJ, Mancuso A, Daikhin E, Nissim I, Yudkoff M, Wehrli S, Thompson CB. Beyond aerobic glycolysis: transformed cells can engage in glutamine metabolism that exceeds the requirement for protein and nucleotide synthesis. *Proc Natl Acad Sci USA.* 2007;104(49): 19345-19350.
35. Ye J, Mancuso A, Tong X, Ward PS, Fan J, Rabinowitz JD, Thompson CB. Pyruvate kinase M2 promotes de novo serine synthesis to sustain mTORC1 activity and cell proliferation. *Proc Natl Acad Sci USA.* 2012;109(18):6904-6909.
36. Kung C, Hixon J, Choe S, et al. Small molecule activation of PKM2 in cancer cells induces serine auxotrophy. *Chem Biol.* 2012;19(9):1187-1198.
37. Vega F, Medeiros LJ, Leventaki V, et al. Activation of mammalian target of rapamycin signaling pathway contributes to tumor cell survival in anaplastic lymphoma kinase-positive anaplastic large cell lymphoma. *Cancer Res.* 2006;66(13):6589-6597.
38. Woessmann W, Peters C, Lenhard M, et al. Allogeneic haematopoietic stem cell transplantation in relapsed or refractory anaplastic large cell lymphoma of children and adolescents—a Berlin-Frankfurt-Münster group report. *Br J Haematol.* 2006;133(2):176-182.
39. Katayama R, Khan TM, Benes C, et al. Therapeutic strategies to overcome crizotinib resistance in non-small cell lung cancers harboring the fusion oncogene EML4-ALK. *Proc Natl Acad Sci USA.* 2011;108(18):7535-7540.